

ENHANCED OH IN C-TYPE SHOCK WAVES IN MOLECULAR CLOUDS

MARK WARDLE

Special Research Centre for Theoretical Astrophysics,
University of Sydney, NSW 2006, Australia*Submitted to Ap. J. Lett.*

ABSTRACT

Cosmic-ray and X-ray ionisations in molecular gas produce a weak far-ultraviolet flux through the radiative decay of H₂ molecules that have been excited by collisions with energetic electrons (the Prasad-Tarafdar mechanism). I consider the effect of this dissociating flux on the oxygen chemistry in C-type shocks.

Typically a few percent of the water molecules produced within the shock front are dissociated before the gas has cooled to 50 K. The resulting column density of warm OH rises from 10¹⁵ to 10¹⁶ cm⁻² as the ionisation rate is increased from 10⁻¹⁷ s⁻¹ (typical of dark clouds) to 10⁻¹⁵ s⁻¹ (adjacent to supernova remnants). These column densities produce substantial emission in the far-infrared rotational transitions of OH, and are consistent with the OH/H₂O ratios inferred from *ISO* observations of emission from molecular shocks. For high ionisation rates the column of warm OH is sufficient to explain the OH(1720 MHz) masers that occur where molecular clouds are being shocked by supernova remnants.

The predicted abundance of OH throughout the shock front will enable C-type shocks to be examined with high spectral resolution through radio observations of the four hyperfine ground state transitions of OH at 18 cm and heterodyne measurements of emission in the FIR (e.g. from *SOFIA*)

Subject headings: MHD — masers — molecular processes — shock waves — ISM: molecules — supernova remnants

1. INTRODUCTION

The energetic electrons produced by cosmic-ray and X-ray ionisations in molecular clouds collisionally excite the Lyman and Werner bands of H₂. The subsequent radiative de-excitations generate a weak flux of far-ultraviolet (FUV) photons capable of dissociating many molecular species (Prasad & Tarafdar 1983). Models of chemistry in C-type shock waves have neglected the internally generated FUV photons, which are able to dissociate $\gtrsim 1\%$ of each shock-produced molecular species before the gas cools to 50 K. Although this does not significantly modify the abundances of the parent species, the relatively small abundance of a dissociation product may be of interest. A particularly important example is the dissociation of water to form OH. It is well-established that H₂O is formed efficiently from OI in the hotter part of the shock front by endothermic reactions once $T \gtrsim 400$ K (Draine, Roberge & Dalgarno 1983; Kaufman & Neufeld 1996). The dissociation of a percent of the water implies an OH abundance $\sim 10^{-6}$, and column densities $\gtrsim 10^{15}$ cm⁻².

This column of warm OH is sufficient to explain the high OH/H₂O abundances inferred from *ISO* observations of shocked molecular gas associated with the HH54 outflow (Liseau et al. 1996), and the supernova remnant 3C391 (Reach & Rho 1998). Enhanced OH abundances associated with shock waves have also been detected at radio wavelengths. OH(1720 MHz) masers are found where supernova remnants are running into molecular clouds (Frail, Goss & Slysh 1994; Yusef-Zadeh, Uchida & Roberts 1995; Frail et al. 1996; Green et al. 1997; Koralesky et al. 1998; Yusef-Zadeh et al. 1999a,b). Population inversion occurs by collisions in warm (40-125 K), moderately dense ($\sim 10^5$ cm⁻³) molecular gas in the absence of a significant FIR radiation field. In addition, a line-of-sight OH column between 10¹⁶ and 10¹⁷ cm⁻² is required for masing to occur (Elitzur 1976; Pavlakis & Kylafis 1986; Lockett, Gauthier & Elitzur 1999). The conditions for masing in this transition are

most likely attained in the cooling tail of a C-type shock wave driven into the cloud by the overpressure within the remnant (Wardle, Yusef-Zadeh & Geballe 1998, 1999; Lockett et al. 1999) provided that sufficient water can be dissociated in the shocked gas before it cools below ~ 50 K.

In this *Letter* I present models of the oxygen chemistry in C-shocks that include dissociations by internally-generated FUV photons. In §2 I outline the physical and chemical processes that are included in the calculations, and results for ionisation rates typical of dark clouds and clouds adjacent to supernova remnants are presented in §3. Warm OH column densities in the range 10¹⁵–10¹⁶ cm⁻² are produced, consistent with the presence of OH(1720 MHz) masers if the shock front harbouring the masers is propagating roughly perpendicular to the line of sight – as is expected because the masing column should have a small line-of-sight velocity gradient. The implications of these results are briefly discussed in §4.

2. SHOCK MODELS

The shock structure is assumed to be steady and plane-parallel with the magnetic field perpendicular to the shock normal. The medium is comprised of neutral and ionised fluids, with the magnetic field frozen into the ionised component and the ionised and neutral components coupled by elastic collisions. The ionisation fraction is low, so the inertia and thermal pressure of the ionised component are neglected.

I follow Kaufman & Neufeld (1996) by writing the magnitude of the drag force per unit volume on the neutrals due to the drift of the charged species as

$$F = \left(\frac{\rho_i}{\rho_{i0}} \right) \frac{\rho v_d^2}{L}, \quad (1)$$

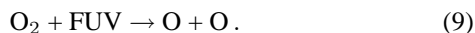
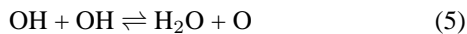
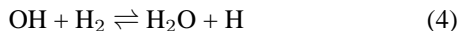
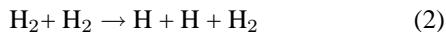
where ρ and ρ_i are the densities of the ion and neutral components, ρ_{i0} is the preshock value of ρ_i , and v_d is the ion-neutral drift speed. The drag force is in the direction of the

ion drift through the neutrals, and there is an equal and opposite force per unit volume exerted on the ions by the neutrals. The coupling lengthscale L is determined by the detailed composition of the ionised fluid, a mixture of molecular and metal ions, electrons and charged grains. The calculation of the upstream ionisation balance by Kaufman & Neufeld (1996) yields $L \approx 10^{17.2} (\zeta/10^{-17} \text{ s}^{-1}) (n_{\text{H}}/10^4 \text{ cm}^{-3}) \text{ cm}$ for the densities of interest here.

The ionisation rate ζ is generally assumed to be due to cosmic rays, but X-rays effect molecular gas similarly (e.g. Maloney, Hollenbach & Tielens 1996) so both ionisation sources are notionally lumped together here. The cosmic-ray and X-ray ionisation rates depend on the environment: in dark clouds the standard interstellar cosmic-ray flux yields $\zeta \sim 10^{-17} \text{ s}^{-1}$, whereas $\zeta \sim 10^{-15} \text{ s}^{-1}$ in molecular gas adjacent to supernova remnants. For example, for a remnant characterised by $L_X = 10^{36} \text{ ergs s}^{-1}$ and a radius of 10 pc, $\zeta \sim 3 \times 10^{-16} \text{ s}^{-1}$ (see §4). The cosmic-ray ionisation rate may also be of this order if the low-energy cosmic ray flux is increased by a factor of 100 over the local interstellar value, as seems to be the case for GeV cosmic rays (Esposito et al. 1996). I therefore consider ionisation rates in the range 10^{-17} – 10^{-15} s^{-1} .

The ambipolar diffusion heating rate per unit volume, neglecting the heat capacity and radiative cooling by the ionised fluid, is Fv_d ; heating by PdV work, and ionisations are also included. Cooling is assumed to occur by collisional dissociation and vibrational transitions of H_2 (Lepp & Shull 1982), and by rotational transitions of H_2 , H_2O , and CO (Neufeld & Kaufman 1993; Neufeld, Lepp & Melnick 1995).

The shock models include a simple reaction network sufficient to follow the oxygen chemistry:



Rates for collisional dissociation of H_2 were obtained from Lepp & Shull (1982); and vibrationally cold rate coefficients for (3)–(6) were taken from Wagner & Graff (1987) apart from their forward rate for (5) which is ill-behaved below 300 K – the rate coefficient from the RATE95 database (Millar, Farqhar & Willacy 1997) is adopted instead. Photodissociation rates for H_2O , OH and O_2 by internally-generated FUV photons were obtained from Gredel et al. (1989).

I adopt shock parameters consistent with the OH(1720 MHz) observations towards W28, W44, and IC443, which imply post shock densities $\sim 10^5 \text{ cm}^{-3}$, and Zeeman field strengths $\sim 0.3 \text{ mG}$ (Claussen et al 1997): a shock speed 25 km s^{-1} , preshock density $n_{\text{H}} = 10^4 \text{ cm}^{-3}$ and preshock magnetic field strength $100 \mu\text{G}$.

3. RESULTS

The shock structure for an ionisation rate $\zeta = 10^{-17} \text{ s}^{-1}$, typical of cosmic-ray ionisation in molecular clouds, is presented in the top panel of Fig. 1. The velocities are plotted in the shock frame, in which the shock is stationary, with

the unshocked gas flowing in from $z < 0$ at the shock speed (i.e. 25 km s^{-1} , being decelerated within the shock front and departing downstream towards $z > 0$). The middle panel shows the chemical abundances obtained when dissociations by internally-generated FUV photons are neglected. As has been found previously (Draine et al 1983; Kaufman & Neufeld 1996) the preshock atomic oxygen is almost entirely incorporated into water, with OH appearing briefly as an intermediate step. For comparison, the lower panel shows the effect of including dissociations by internally-generated FUV. The overall chemistry is not drastically affected, but dissociation of water produces an increasing abundance of OH downstream, with a significant column having accumulated by the time the gas has cooled to 50 K. Note also the gradual reappearance of OI downstream through the dissociation of OH and O_2 .

The effect of raising the ionisation rate to $3 \times 10^{-16} \text{ s}^{-1}$, as produced by X-rays in a molecular cloud adjacent to a SNR, is illustrated in Fig. 2. The ionisation fraction of the preshock gas is increased by a factor of $\sqrt{30}$, reducing the thickness of the shock transition and the time scale for gas to flow through the shock front by the same factor. The peak neutral temperature increases because the energy dissipated in the shock must be radiated away on a shorter time scale. Heating associated with ionisations, which is unimportant within the shock front, increases 30-fold and so the final postshock temperature increases slightly. The photodissociation rate is increased 30-fold, with a concomitant increase in the production of OH and OI.

Fig. 3 summarises the production of OH within the shock models by plotting the run of OH column density with temperature within the shock front for different ionisation rates. An initial ‘burst’ of OH column is produced as oxygen is rapidly converted to water in the high-temperature portion of the shock front. The column produced during this phase decreases as the ionisation rate is increased because the OH destroying forward reaction in (4) is strongly temperature dependent, and the temperature within the shock rises more rapidly for high ionisation rates because of the increase in the rate of ambipolar diffusion heating. If the FUV dissociation is neglected no more OH is produced (dashed curves); otherwise OH starts to be produced once the temperature of the shocked gas has dropped sufficiently so that the forward reaction in (4) has slowed sufficiently to permit photodissociations to become effective. For high ionisation rates the increase in the photodissociation rate ($\propto \zeta$) is partially offset by the decrease in flow time scale ($\propto \zeta \text{ sup}^{-1/2}$); thus $N_{\text{OH}} \propto \zeta \text{ sup}^{1/2}$ in the cooling gas.

4. DISCUSSION

The line-of-sight column density of warm OH through a C-type shock is $N_{\text{OH}} \sec \theta$ where θ is the angle between the shock normal and the line of sight. For $\zeta \gtrsim 10^{-16} \text{ s}^{-1}$ and $\theta \gtrsim 80^\circ$, N_{OH} is sufficient to permit the formation of OH(1720 MHz) masers, thus typical X-ray fluxes near SNRs are able to produce the warm OH column necessary for OH(1720 MHz) masers.

Lockett et al. (1999) have argued that the X-ray flux from SNRs is typically a thousandth of that required to indirectly produce the OH column density required to produce the masers. Two of the discrepant factors of ten arise because they require X-rays to dissociate *all* of the water rather than the $\sim 1\%$ that is actually necessary. The remaining factor of ten can be traced to the conversion from X-ray energy flux F_X to ionisation rate. Both Wardle et al. (1998) and Lockett et al. (1999) used the conversion $\zeta (\text{s}^{-1}) \approx 3 \times 10^{-14} F_X (\text{erg cm}^{-2} \text{ s}^{-1})$ (Maloney

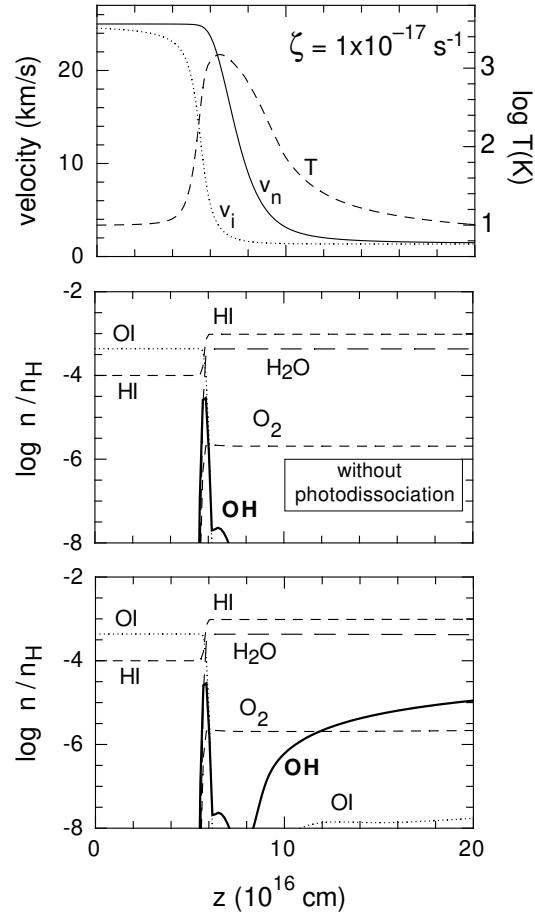


FIG. 1.— (*Top panel:* velocity and temperature profile (the temperature scale is on the right) of a 25 km s^{-1} C-type shock propagating into gas with $n_{\text{H}} = 10^4 \text{ cm}^{-3}$ and $B_0 = 100 \mu\text{G}$. The X-ray + cosmic ray ionisation rate is assumed to be $\zeta = 10^{-17} \text{ s}^{-1}$ (see text). *Middle panel:* oxygen chemistry in the absence of dissociation by the FUV radiation field induced by ionisations. *Lower panel:* oxygen chemistry with dissociations included.

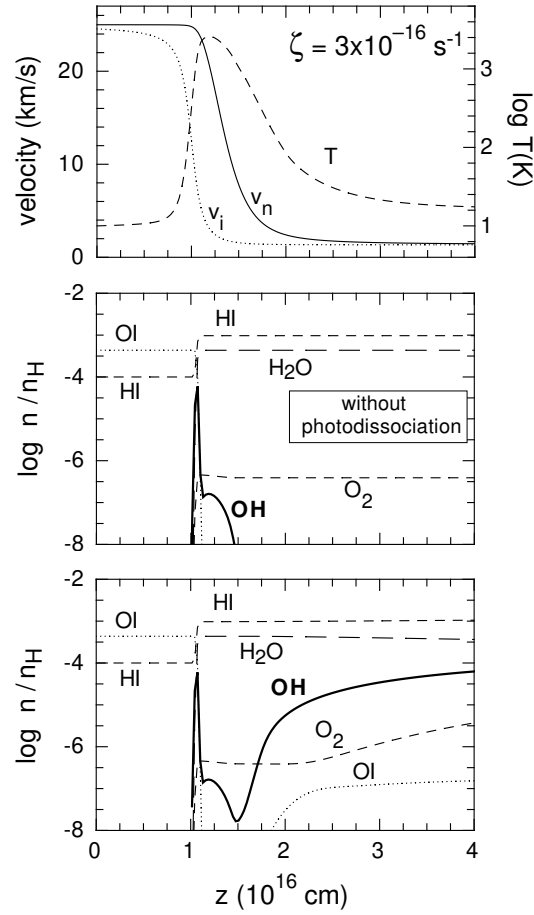


FIG. 2.— As for Fig 1, but for an ionisation rate $\zeta = 3 \times 10^{-16} \text{ s}^{-1}$, typical of molecular clouds adjacent to supernova remnants.

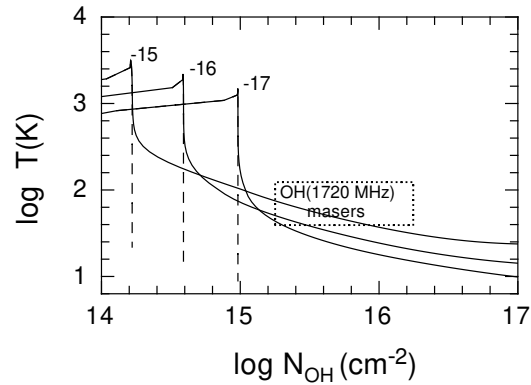


FIG. 3.— *Solid*: OH column density versus temperature within C-type shock models with $v_s = 25 \text{ km s}^{-1}$, $n_H = 10^4 \text{ cm}^{-3}$, and $B_0 = 100 \mu\text{G}$. The curves are labelled by $\log \zeta$ (s⁻¹). *Dashed*: The same, but with photodissociations neglected. The dotted box indicates the conditions necessary for 1720 MHz masers to form.

et al. 1996), but this assumes a hard X-ray spectrum appropriate to AGNs. The softer ($\bar{E} \sim 1$ keV) spectrum from the hot gas in SNRs produces more ionisations per unit X-ray luminosity, as ionisations are dominated by low-energy X-ray photons. In this case, $\zeta \approx N_e \sigma F_X$ where $N_e \approx 30 \text{ keV}^{-1}$ is the mean number of primary and secondary electrons produced by the absorption of unit energy, $\sigma \approx 2.6 \times 10^{-22} \text{ cm}^{-2}$ is the photoabsorption cross-section per hydrogen nucleus at 1 keV, and $F_X = L_X/4\pi R^2$. With $L_X = 10^{36} \text{ erg s}^{-1}$ and $R = 10 \text{ pc}$, this yields $\zeta \approx 4.6 \times 10^{-16} \text{ s}^{-1}$ provided that the hydrogen column density $N_H \lesssim 10^{22} \text{ cm}^{-2}$.

The enhancement of OH described in this *Letter* permits the structure and kinematics of C-type shock waves to be studied through the modelling of the excitation of OH throughout the shock front, and the calculation of emission and absorption line profiles. Supernova remnants with associated 1720 MHz masers (Frail et al. 1994, 1996; Yusef-Zadeh et al. 1995,

1996, 1999a,b; Green et al. 1997; Koralesky et al. 1998) are obvious observational targets. At radio wavelengths, the four ground-state transitions at 1612, 1665, 1667 and 1720 MHz can be observed with sub-km/s velocity resolution in absorption against the background continuum from the remnant. For example, W28 shows extended OH absorption around the OH maser positions (Pastchenko & Slysh 1974; Claussen et al. 1997). The predicted warm OH column within C-type shocks implies substantial far-infrared emission in low-lying OH rotational transitions. This will, for example, be easily detectable by the GREAT heterodyne spectrometer planned for SOFIA, an instrument that will be capable of 0.1 km/s or better velocity resolution.

The Special Research Centre for Theoretical Astrophysics is funded by the Australian Research Council under its Special Research Centres programme.

REFERENCES

- Claussen, M. J., Frail, D. A., Goss, W. M. & Gaume, R. A. 1997, *ApJ*, 489
 Draine, B. T., Roberge, W. G. & Dalgarno, A. 1983, *ApJ*, 264, 485
 Elitzur, M. 1976, *ApJ*, 203, 124
 Esposito, J. A., Hunter, S. D., Kanbach, G. & Sreekumar, P. 1996, *ApJ*, 461, 820
 Frail, D. A., Goss, W. M., Reynoso, E. M., Giacani, E. B., Green, A. J. & Otrupcek, R. 1996, *AJ*, 111, 1651
 Frail, D. A., Goss, W. M. & Slysh, V. I. 1994, *ApJ*, 424, L111
 Gredel, R., Lepp, S., Dalgarno, A. & Herbst, E. 1989, *ApJ*, 347, 289
 Green, A. J., Frail, D. A., Goss, W. M. & Otrupcek, R. 1997, *AJ*, 114, 2058
 Kaufman, M. J. & Neufeld, D. A. 1996, *ApJ*, 456, 611
 Koralesky, B., Frail, D. A., Goss, W. M., Claussen, M. J. & Green, A. J. 1998, *AJ*, 116, 1323
 Lepp, S. & Shull, J. M. 1983, *ApJ*, 270, 578
 Liseau, R., Ceccarelli, C., Larsson, B., Nisini, B., White, G. J., Ade, P., Armand, C., Burgdorf, M., Caux, E., Cerulli, R., Church, S., Clegg, P. E., Digorgio, A., Furniss, I., Giannini, T., Glencross, W., Gry, C., King, K., Lim, T., Lorenzetti, D., Molinari, S., Naylor, D., Orfei, R., Saraceno, P., Sidher, S., Smith, H., Spinoglio, L., Swinyard, B., Texier, D., Tommasi, E., Trams, N. & Unger, S. 1996, *A&A*, 315, L181
 Lockett, P., Gauthier, E. & Elitzur, M. 1999, *ApJ*, 511, 235
 Maloney, P. R., Hollenbach, D. J. & Tielens, A. G. G. M. 1996, *ApJ*, 466, 561
 Millar, T. J., Farquhar, P. R. A. & Willacy, K. 1997, *AASupp*, 121, 139
 Neufeld, D. A. & Kaufman, M. J. 1993, *ApJ*, 418, 263
 Neufeld, D. A., Lepp, S. & Melnick, G. J. 1995, *ApJ Supp*, 100, 132
 Pastchenko, M. I. & Slysh, V. I. 1974, *A&A*, 35, 153
 Pavlakis, K. G. & Kylafis, N. D. 1996, *ApJ*, 467, 300
 Prasad, S. S. & Tarafdar, S. P. 1983, *ApJ*, 267, 603
 Reach, W. T. & Rho, J. 1998, *ApJ*, 507, L93
 Wagner, A. F. & Graff, M. M. 1987, *ApJ*, 317, 423
 Wardle, M., Yusef-Zadeh, F. & Geballe, T. R. 1998, preprint (astro-ph/9804146)
 Wardle, M., Yusef-Zadeh, F. & Geballe, T. R. 1999, in *The Central Parsecs*, eds. H. Falcke et al. in press (astro-ph/9811090)
 Yusef-Zadeh, F., Goss, W. M., Roberts, D. A., Robinson, B. & Frail, D. A. 1999a, *ApJ*, in press
 Yusef-Zadeh, F., Roberts, D. A., Goss, W. M., Frail, D. A. & Green, A. J. 1996, *ApJ*, 466, L25
 Yusef-Zadeh, F., Roberts, D. A., Goss, W. M., Frail, D. A. & Green, A. J. 1999b, *ApJ*, 512, 230
 Yusef-Zadeh, F., Uchida, K. & Roberts, D. A. 1995, *Science*, 270, 1801